CIRP Annals - Manufacturing Technology xxx (2018) xxx–xxx

Contents lists available at ScienceDirect

CIRP Annals - Manufacturing Technology

journal homepage: http://ees.elsevier.com/cirp/default.asp

Precision enhanced electrochemical jet processing

Adam T. Clare *, Alistair Speidel, Ivan Bisterov, Alexander Jackson-Crisp, Jonathon Mitchell-Smith

ACEL, Faculty of Engineering, University of Nottingham, Nottingham, NG7 2RD, UK

Submitted by Professor David Williams, Loughborough University.

ARTICLE INFO

Keywords:
Electrolyte jet
Precision machining
Electrochemical

ABSTRACT

Through electro-physical modification of the electrode gap in electrochemical jet techniques, precision has been shown to be greatly increased. Repeatable kerf widths approaching the diameter of the nozzle are demonstrated and the individual contributing effects are quantified across energy density and length scales. This allows the feature resolution achievable through electrochemical jet processing to be comparable to other surface structuring techniques, albeit with zero thermal loading of the surface. This is applied to demonstrate the machining of complex geometric features, not previously produced by electrolyte jet techniques.

1. Introduction

The use of electrolyte jet-based techniques to generate microscale features in engineering materials has been notably demonstrated by Kunieda et al. [1] and Hackert et al. [2]. Contributions made here have established that the resultant machined feature is characteristic of the energy distribution within the jet. Material response to electrolyte jet techniques is a function of the principle factors of electrolyte type, feedstock precondition, and energy density. Experimentation with these factors has shown that both material removal [3] and surface finish [4] can be manipulated. More recently, the authors have demonstrated three techniques that enhance the precision of electrolyte jet techniques: (i) optimisation of angle of address [5], (ii) use of transitory masking effects [6] and (iii) energy density modulation [7].

Fig. 1 shows a comparison between the traditional machining configuration in which the nozzle is addressed perpendicular to the work, Fig. 1a), and a combined machining mode that may be exploited to enhance precision, Fig. 1b) forming the hypothesis of this work. The advantages of changing the angle of address have been reported. This serves to distort the current density distribution and localise field effects. Response profiles exhibit a smoother finish, with a deeper cut and reductions in the kerf [5].

In addition, it has been demonstrated that formulation of the electrolyte can improve the precision of electrochemical jet processing (EJP). Through the creation of a selective oxidation regime, it is possible to establish a transitory current filtering effect, whereby a doping compound within the electrolyte is preferentially oxidised. Process optimisation can lead to almost complete oxidation of the dopant, creating an energy threshold that must be overcome before anodic dissolution (machining) can occur. Since the periphery of the jet does not exhibit sufficient energy density to overcome this threshold, the kerf width can be reduced. Through the use of iodide-doped electrolytes, a 26% reduction in dissolution kerf has been demonstrated, along with improvements in cut-edge definition [6].

It has also been demonstrated that nozzle profiling can modify the current density distribution, by creating field-focussing features. This allows the resultant kerf profile to be manipulated.

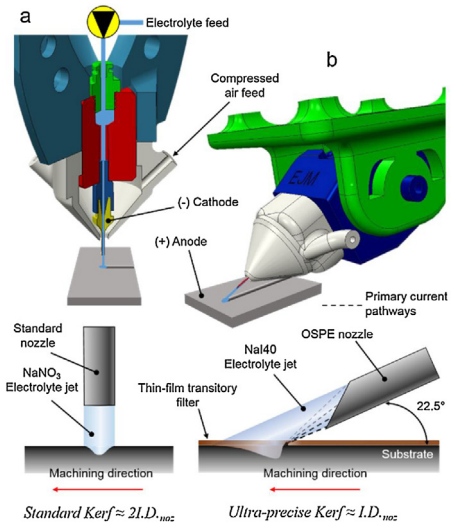

Fig. 1. (a) The conventional perpendicular machining mode (baseline). (b) The contrasting arrangement used here, which exploits nozzle tilting, thin-film transitory filtering and modulation of energy density.

* Corresponding author.
E-mail address: adam.clare@nottingham.ac.uk (T. Clare).

https://doi.org/10.1016/j.cirp.2018.04.086
0007-8506/

Typically, the dissolution kerf in electrochemical jet methods is acknowledged to be defined by the stagnation region of the impinging jet flow field, before transforming into the radial wall jet region. This creates a highly resistive thin-film layer where dissolution is inhibited. This is defined by $r/d < 1$. Where r is the radial distance from the stagnation point and d, the nozzle internal diameter [8]. Reduction of the dissolution kerf beyond this represents a significant process change through disassociation of the dissolution regime, from the hydrodynamic regime developed by the impinging jet stream.

It is proposed that through a combination of these novel approaches to EJP, the compound effect of each process enhancement will be greater than the individual contributions. This would enable the generation of fine-featured geometries desirable in micromachining applications.

2. Materials and methodology

2.1. Experimental apparatus

In this study a purpose built EJP apparatus was used. Compared to the original definition of this equipment [7], an enhanced tool holding system was developed, allowing the nozzle angle to be indexed relative to the work. Two orientations of the nozzle were investigated here (90° and 22.5°, relative to the workpiece, see Fig. 1). The apparatus was used to create striations at two current densities (200 and 400 A/cm^2). Demonstration of the effects at two different current densities is critical since material removal phenomena adopt distinct regimes with increasing current density. Jet velocity and nozzle traverse speed remained constant throughout at 25 m/s, 0.5 mm/s respectively. Inter-electrode gap was initially set at 0.5 mm where the nozzle is perpendicular to the workpiece and 0.3 mm where the nozzle is inclined. The difference due to the increasing jet path when the jet address is inclined leading to increased resistance if not amended.

Two nozzle types were used in this study, a conventional flat tip and an off-centre single point element (OSPE). The latter is a chamfered version of the conventional nozzle manufactured using wire EDM (see Fig. 1b). Experimental trials were carried out both individually and combining the variables detailed. (see Table 1).

Beginning with the baseline standard configuration, augmentations were made in a piece-wise manner, including the application of an electrolyte, which exhibits the transitory masking effect (see Section 2.3). Machining effect comparison was undertaken using nozzles of equivalent I.D. (250 μm), stray cutting reduction was appraised using a 60 μm nozzle I.D., and capability demonstration was undertaken using a 150 μm nozzle I.D. This shows the scalability of augmentations hereby proposed.

Table 1
Experimental configuration for evaluating the compound effect of transitory masking, nozzle profiling and angle of address upon machining precision.

Baseline	Std. nozzle, standard electrolyte (MME = 0)
Mode 1 (electrolyte)	Std. nozzle, NaI40 electrolyte
Mode 2 (nozzle)	OSPE nozzle, standard electrolyte
Mode 3 (Angle of address)	Std. nozzle, standard electrolyte, 22.5° angle
Mode 4 (Combined)	OSPE nozzle, NaI40 electrolyte, 22.5° angle

2.2. Attributing response

To demonstrate mode-specific enhancements in machining performance, a composite metric was defined for quantification. This allows simply comparison of the influence of the differing machining modes on overall profile improvement and their effect on individual areas of the response profile. Machining mode effect (MME) is proposed here as an appropriate way of defining this, through an amalgamation of kerf width (K), depth of cut (D), feature to surface shoulder precision (P), and cut-wall slope (CWS) (see Fig. 2 for description of metrics). For an ideal machining scenario, K should be minimised, while D, P and CWS should be maximised. An increased MME represents an improved set of machining conditions and thus precision.

$$MME = \left[\frac{(K_{baseline} - K_{mode\ 1})}{K_{baseline}}\right] + \left[\frac{(D_{mode\ 1} - D_{baseline})}{D_{baseline}}\right] + \left[\frac{(P_{mode\ 1} - P_{baseline})}{P_{baseline}}\right] + \left[\frac{(CWS_{mode\ 1} - CWS_{baseline})}{CWS_{baseline}}\right] \quad (1)$$

Utilising this method, a direct comparison of machining configurations can be undertaken against a baseline (MME = 0). In addition, through consideration of each configuration in turn, the response of the machined profile can be unambiguously defined.

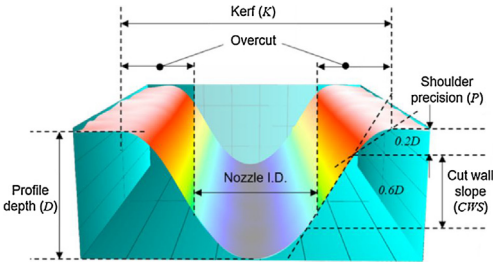

Fig. 2. Using a typical cut profile the metrics used to define geometrical impact of varying machining modes and MME equation are shown. Both Precision (P) and cut-wall-slope (CWS) are slopes produced in rise over run format (μm/μm).

2.3. Materials and electrolytes

The high-temperature aerospace alloy Inconel 718 was used as the workpiece throughout the experimental study. Widely used in creep and fatigue sensitive applications, the athermal machining of this material for surface texturing, where integrity is ensured, is critical. Additional demonstration of the enhanced resolution was undertaken using shim-steel (100 μm), where through features are created.

Two electrolytes were used in this study, at equimolar ionic strength (2.3 M). A conventional EJP electrolyte, $NaNO_3$, (standard electrolyte), was compared with an iodide-doped nitrate-based electrolyte, $NaNO_3$ 1.38 M: NaI 0.92 M, (NaI40). The transient masking effect has previously been shown to be independent of electrolyte conductivity ($NaNO_3$ 136.6 ms/cm^{-1}, NaI40 149.4 ms/cm^{-1}, at 23.0 °C), within the ranges tested.

2.4. Characterisation apparatus

In order to measure the attributes K, D, CWS and P, a focus-variation (FV) microscope was used (Alicona, G5 Infinitefocus, 50× objective). Scanning electron microscopy (SEM) in secondary electron mode was also undertaken on specimens to evaluate kerf edge effects associated with transitory masking (Philips XL30 and Jeol 6060LV).

3. Results

3.1. Evaluating compound effects

Through the application of the MME (1), it is possible to assess the contributions each mode makes to the overall improvement of the profile geometry being analogous with increased precision. Considering Fig. 3, the individual effect that each mode has on K, D, P, and CWS, can be compared to the increase in applied current density. The overall effects are reduced as J is increased. From the 200 A/cm^2 trials, the effect of combining all the modes slightly reduces the overall effectiveness on geometry improvement. This is due to the application of NaI40, whereby a negative effect results, from a reduction in the maximum depth. This correlates with the depth reduction in the combined mode 4. However, the inclusion of NaI40 does have a further effect of increasing the feature-to-surface

Please cite this article in press as: Clare AT, et al. Precision enhanced electrochemical jet processing. CIRP Annals - Manufacturing Technology (2018), https://doi.org/10.1016/j.cirp.2018.04.086